CellPress
OPEN ACCESS

Trends in
Biotechnology

Research Article

Engineered coatings containing cyclic peptides from cyanobacteria delay the development of a stable macrofouling community

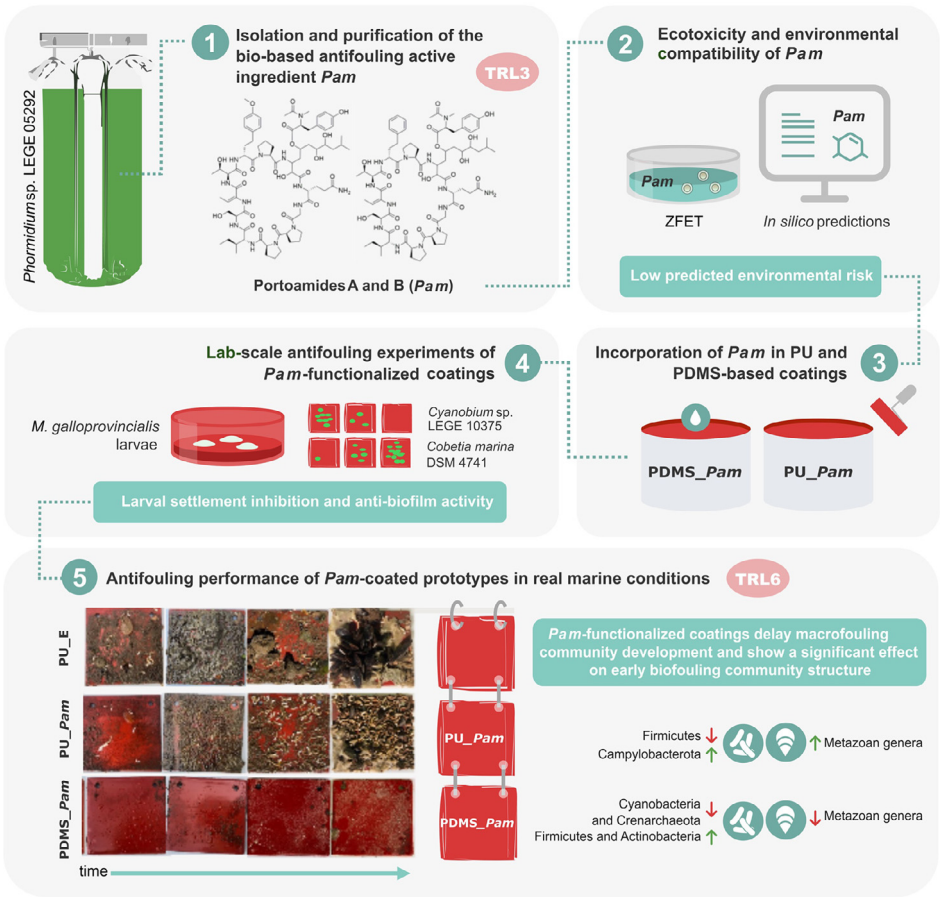

Bio-based antifouling coatings incorporating cyanobacterial natural products inhibit biofilm formation and mussel larval settlement at lab scale, outperforming a commercial biocide under real marine conditions by promoting an antifouling–effective biome. This technology provides a promising route toward sustainable, eco-safe antifouling solutions with potential applications across marine ecological management.

Catarina Gonçalves, Sandra Pereira, Isabel B. Oliveira, Marco Preto, Tiago Ribeiro, João Morais, Luciana C. Gomes, Maria João Romeu, Miguel Semedo, Filipe J. Mergulhão, Vitor Vasconcelos, Elisabete R. Silva, Joana R. Almeida

jalmeida@ciimar.up.pt (J.R. Almeida).

Highlights

Marine biofouling imposes major ecological and economic burdens, driving the search for sustainable antifouling strategies.

We engineered bio-based coatings functionalized with the natural cyclic peptides portoamides A and B (*Pam*), derived from cyanobacteria.

Pam-functionalized coatings inhibited mussel larval settlement, disrupted biofilm formation, and outperformed a commercial biocide under real marine conditions.

This proof-of-concept advances antifouling technology from lab-scale (Technology Readiness Level 3) to field-validated prototypes (Technology Readiness Level 6), marking a key step toward eco-safe marine coatings.

Trends in Biotechnology, May 2026,
Vol. 44, No. 5
https://doi.org/10.1016/j.tibtech.2025.11.018

© 2025 The Author(s). Published by Elsevier Ltd. This is an open access article under the CC BY license (http://creativecommons.org/licenses/by/4.0/).

Check for updates

Trends in Biotechnology

CellPress OPEN ACCESS

Research Article

Engineered coatings containing cyclic peptides from cyanobacteria delay the development of a stable macrofouling community

Catarina Gonçalves [1,2,#], Sandra Pereira [1,2,#], Isabel B. Oliveira [1], Marco Preto [1], Tiago Ribeiro [1], João Morais [1], Luciana C. Gomes [3], Maria João Romeu [3], Miguel Semedo [1], Filipe J. Mergulhão [3], Vitor Vasconcelos [1,2], Elisabete R. Silva [4,5], and Joana R. Almeida [1,*]

Biofouling—the adhesion of organisms and their byproducts to submerged surfaces—poses economic and environmental challenges, highlighting the need for sustainable antifouling solutions. This study reports a proof-of-concept investigation into the environmental compatibility and field validation of natural cyclic peptides portoamides A and B (*Pam*) as a bio-based antifouling alternative. *Pam* have demonstrated antifouling activity by inhibiting mussel larval settlement and disrupting biofilm formation. Herein, the antifouling performance of *Pam*-engineered coatings was evaluated through anti-settlement, anti-biofilm, as well as marine field tests. Lab-scale tests revealed that *Pam*-based coatings (0.7 wt%) effectively reduced biofilm thickness, surface coverage, and mussel larval settlement. Field trials showed that *Pam*-functionalized coating prototypes outperformed a commercial biocide in use (Econea®), delaying macrofouling community establishment and contributing to enhanced antifouling effectiveness. Overall, this work supports further development of antifouling engineered systems using *Pam*, representing a significant technological advance (from Technology Readiness Level 3 to 6) toward sustainable marine coating systems.

Technology readiness

Pam-functionalized coatings, a bio-based antifouling technology engineered to modulate early-stage biofouling community colonization and delay the establishment of macrofouling organisms, have reached the Technology Readiness Level (TRL) 6. This technology has been successfully tested under both laboratory and relevant marine conditions, demonstrating high effectiveness in preventing biofilm formation and mussel larval settlement at lab-scale, as well as sustained antifouling performance in marine field trials. To progress toward higher TRLs, key challenges include optimizing cost-effective, large-scale production of the cyanobacterial metabolites, demonstrating efficacy across diverse marine environmental settings worldwide, and adapting coating matrices to meet the needs of different end users. Reaching these milestones will support the transition toward next-generation, eco-friendly antifouling technologies.

Introduction

Marine biofouling is a natural dynamic process that refers to the reversible or irreversible colonization and adhesion of a diversity of marine organisms, such as bacteria, algae, and invertebrates, and their byproducts on virtually all submerged structures [1]. The formation of biofilms and **early-stage biofouling communities** (see Glossary) relies on the surrounding marine community structure, but is shaped by the nature of the colonization substrates, as their intrinsic properties may inhibit certain types of bioadhesion. Still, the first colonizers that successfully settle on a given substrate play a crucial role in driving subsequent colonization. **Microbial cues**, including secondary metabolites and macromolecular structures, mediate interactions between microorganisms, other benthic organisms, and their environment, ultimately defining the composition and dynamics of the biofouling community [2].

Established biofouling communities represent an economic burden to ocean-related industries, with aquaculture and shipping being particularly affected [3,4]. Preventive measures used to date, namely the continuous use and release of aggressive antifouling (AF) agents into the marine environment, constitute an environmental problem, contributing to the loss of marine biodiversity and damage to ecosystems [5]. Traditional **antifouling coatings** have raised significant environmental concerns due to the toxicity of their biocidal components [6]. Some biocides were banned

[1]CIIMAR/CIMAR LA, Interdisciplinary Centre of Marine and Environmental Research, University of Porto, Terminal de Cruzeiros do Porto de Leixões, Matosinhos 4450-208, Portugal
[2]Department of Biology, Faculty of Sciences, University of Porto, Rua Campo Alegre s/n, Porto 4169-007, Portugal
[3]LEPABE – Laboratory for Process Engineering, Environment, Biotechnology and Energy, ALiCE – Associate Laboratory in Chemical Engineering, Faculty of Engineering, University of Porto, Rua Dr. Roberto Frias, 4200-465 Porto, Portugal

© 2025 The Author(s). Published by Elsevier Ltd. This is an open access article under the CC BY license (http://creativecommons.org/licenses/by/4.0/).

[4]BioISI – Biosystems & Integrative Sciences Institute, Faculdade de Ciências, Universidade de Lisboa, Campo Grande, Lisboa 1749-016, Portugal
[5]Departamento de Química e Bioquímica, Faculdade de Ciências, Universidade de Lisboa, Campo Grande, 1749-016 Lisboa, Portugal
[#]These authors contributed equally

*Correspondence:
jalmeida@ciimar.up.pt (J.R. Almeida).

[e.g., Tributyltin (TBTs)] and the Biocidal Products Regulation (BPR) EU 528/2012 was issued, forcing EU members to invest in the development of environmentally compatible AF strategies [7–9]. Current AF biocide-based coating technologies (95% of total market size) still rely on the controlled release of biocides (primarily copper- or metal-based) from the coating matrix. These remain effective for 6 months to 5 years [1,10] and are harmful to marine ecosystems. Fouling release systems (5% market share) are coatings made of crosslinked polydimethylsiloxane (PDMS) matrix and/or doped with 6–10% of PEG [poly(ethylene glycol)]–PDMS copolymer [11], which do not rely on biocidal action. Such systems are not specifically regulated, despite the toxicity of their leachates (microparticles), which seems to be comparable to conventional biocide-release AF coatings [12]. The growing recognition of these detrimental effects has encouraged research and development of environmentally compatible alternatives [13–15]. Still, fully eco-friendly solutions are not yet available, and the market continues to rely on copper and booster biocides-based polluting coatings [1].

Several submerged biological surfaces provide effective protection against **epibiosis** [16]. Such natural strategies in the marine environment include chemical defense through the production of bioactive metabolites, structural and textural arrangement of outer surfaces, microbial symbiosis, among others [2,17,18]. Such bio-based strategies hold significant promise as inspiration for the next generation of AF technologies, offering both effectiveness and environmental compatibility [19]. Marine-derived natural products have been demonstrating targeted AF efficacy [9,20–22]. Examples include zosteric acid and 6-bromoindole-3-carbaldehyde, identified in the eelgrass (*Zostera marina*) and coral-associated bacterium *Acinetobacter* sp., respectively [23,24], synoxazolidinones A and C and pulmonarins A and B from the sub-arctic ascidian *Synoicum pulmonaria* [25], barettin from the sponge *Geodia barretti*, and phidianidines A and B from the nudibranch gastropod *Phidiana militaris* [26,27]. However, a nonbiocidal broad-spectrum solution for commercial use is yet to be reached. Recent perspectives point out that engineering surface features that interfere with organisms' sensing, thereby modulating the adherence of specific bacterial biofilms and potentially preventing exponential community development, should be a research priority [28]. High-throughput sequencing (HTS) studies have shown that commercial AF coatings are associated with a lower diversity of early colonizing communities [29,30], but the potential of bio-based active principles to create such privileged stable AF communities is still unexplored.

Our group has recently assessed the potential of the cyanobacterial cyclic dodecapeptides, portoamides A and B (*Pam*, Figure 1), as a bio-based active ingredient in AF compositions [31]. This natural ingredient (*Pam*), isolated from the cyanobacterium *Phormidium* sp. LEGE 05292, showed high effectiveness in the prevention of mussel larvae settlement and was also active toward marine biofouling bacterial strains, while not showing toxicity toward both target and nontarget species [31].

Here, we further explored the potential of *Pam* as a valuable antifouling (AF) ingredient to advance from an early conceptual experimental level [Technology Readiness Level (TRL) 3] to near-application in a relevant environment readiness (TRL 6), establishing an effective and environmentally responsible alternative to conventional coatings. We hypothesized that *Pam*-coated surfaces could foster the colonization of a specific biofouling community capable of maintaining a stable, low-diversity, and **AF-effective biome** in real marine conditions, while posing minimal environmental risk to marine ecosystems. To reach this, pilot-scale production and incorporation of *Pam* in commercial polyurethane (PU) and silicone (PDMS)-based marine coatings were carried out. The produced coatings were evaluated through laboratory-scale experiments and proof-of-concept trials conducted under real sea conditions at Leixões Port (Portugal). *In situ* tests

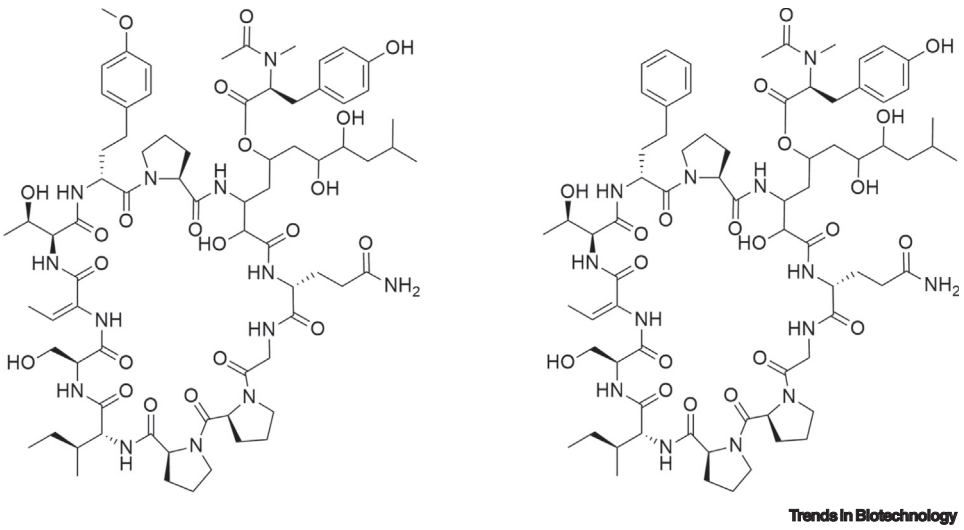

Figure 1. Portoamides A (left) and B (right).

investigated the composition and diversity of microbial and early macrobiota communities through *in vivo* macroscopic inspections and HTS analyses. The environmental risk of *Pam* was further explored, including predictive risk parameters and potential leaching from the prepared coating formulations. This integrated approach illuminated our understanding of the biological diversity within early-stage biofouling communities associated with bio-based AF surfaces, contributing to the development of more sustainable AF technologies.

Results and discussion

Environmental compatibility of the naturally produced active ingredient *Pam*

The cyanobacterial AF bioactive ingredient *Pam* was produced under optimized culture conditions, yielding 1.1 g of purified material over 6 months (Figure S1 in the Supplemental information online). Its environmental compatibility and AF behavior in coatings were evaluated. Given the previous indications of the suitable ecotoxicological profile of *Pam* [32,33], the Fish Embryo Acute Toxicity test (OECD guideline 236) was performed to assess toxicity at higher biological levels and estimate risk parameters in ecologically relevant scenarios. Treatments were compared to a 0.1% Dimethyl sulfoxide (DMSO) control, a safe concentration in Zebrafish Embryo Acute Toxicity Test (ZFET) [34]. The median lethal concentration (LC_{50}) for zebrafish embryos was 6.25 (6.071–6.43, 95% CI) mg l^{-1} (Figure S2 in the Supplemental information online). This was lower than reported values for the microalgae *Chlorella vulgaris* (IC_{50} = 12.8 mg l^{-1}), *Ankistrodesmus falcatus* (IC_{50} = 24.7 mg l^{-1}), and *Chlamydomonas reinhardtii* (IC_{50} = 12.6 mg l^{-1}) [33], or on *Artemia salina*, which showed no mortality up to 24.4 mg l^{-1} [32]. The experimental LC_{50} (6.254 mg l^{-1}) was compared to ECOSAR's estimated LC_{50} for *Danio rerio* (1.4×10^5 mg l^{-1}) to determine the Toxic Ratio (TR). A TR of 1.66×10^7 exceeded the threshold of 10, supporting a specific mode of action rather than baseline toxicity [19,35]. *Pam* had a low log K_{ow} (–5.488), indicating minimal bioconcentration potential. However, as ECOSAR is unreliable for molecular weights greater than 1000 g mol^{-1}, which is the case of *Pam* (Molecular weight (MW) of portoamide A ≈ 1532 g mol^{-1} and B ≈ 1502 g mol^{-1}), results remain indicative [35].

Quantitative risk assessment compared the predicted environmental concentration (PEC, from MAMPEC; Table S4 in the Supplemental information online) to the predicted no-effect concentrations (PNEC from zebrafish LC50). A PEC/PNEC > 1 suggests ecological risk [36]. Simulated environmental

Glossary

AF-effective biome: surface-associated biotic assemblage shaped by the presence of antifouling cues.

Antifouling coatings: engineered surface treatments applied to structures intended for submersion to prevent or reduce the settlement and growth of biofouling organisms, by providing physical and chemical surface properties that deter adhesion and biofilm formation, thereby enhancing material durability, operational efficiency, and environmental performance.

Early-stage biofouling communities: initial multispecies assemblages dominated by microorganisms—such as bacteria, microalgae, and fungi—along with larval stages of macroorganisms that rapidly colonize submerged surfaces. Their composition, succession, and functional interactions are shaped by environmental factors and substrate characteristics, while their intrinsic biochemical activity conditions the surface and drives subsequent stages of biological colonization.

Epibiosis: colonization of a living host's surface by other organisms, resulting in the formation of surface-associated communities that can influence the host's ecological and functional processes.

Microbial cues: biochemical signals or byproducts produced by microorganisms—such as metabolites, extracellular polymeric substances, or surface-bound molecules—that modulate the behavior, settlement, or developmental processes of other organisms within a biofilm or biofouling community.

concentrations obtained here (Table S4) were significantly lower than those of known antifouling compounds, such as tralopyril (Econea®) and tributyltin [37]. A comparative analysis between *Pam* and a set of reference AF biocides and natural alternatives, regarding persistence, bioaccumulation, and toxicity (PBT criteria), together with regulatory status, key biological effects, and risk characterization data (Table S5 in the Supplemental information online), shows that traditional AF biocides such as tributyltin and copper exhibit high persistence, strong bioaccumulation potential, and significant toxicity across trophic levels, resulting in historically high environmental risks [38,39]. Tralopyril, used in this study as a reference compound under its commercial designation Econea®, as well as DCOIT, although approved under the Biocidal Products Regulation (BPR), exhibit elevated toxicity and a high ecological risk (PEC/PNEC > 1) [40–43]. In turn, medetomidine seems to fulfill the requirements of a good biocide (low persistence, rapid elimination rate, and low ecological risk) [44–46] although more studies are needed to further evaluate its potential effect on certain organisms. In contrast, naturally derived compounds with available ecotoxicological data, such as capsaicin and *Pam*, present a more favorable ecotoxicological profile, characterized by low acute toxicity, low persistence, and limited bioaccumulation potential. Specifically, *Pam* demonstrated no mortality in *Artemia salina*, reversible effects on mussel larvae settlement, and the highest ZFET LC_{50}, indicating an overall low hazard potential for nontarget organisms. Recent antifouling candidates of natural origin—such as barettin [47,48], phidianidine A/B [27,49], adenosine and 2′-deoxyadenosine [50], and actinobacterial metabolites including napyradiomycins [51], madeirone, and neomarinone [52]—also seem to show low acute toxicity, reinforcing the environmental compatibility trend observed for natural product-based antifoulants. However, data on the PBT criteria are still missing to fully assess the toxicity of these compounds. Among the selected natural compounds, only nocuolin A exhibited higher ecological risk, limiting its immediate potential as an environmentally compatible option [53].

Taken together, this comparative framework highlights that *Pam* combines strong biological efficacy with an improved environmental safety margin, supporting its potential as a sustainable AF candidate relative to both currently used and emerging biocides.

Bio-based coating formulations containing *Pam* preserve the inherent anti-biofilm and larval settlement inhibition potential

Commercial polyurethane (PU) and polydimethylsiloxane (PDMS)-based marine polymeric matrices were used to optimize coating formulations incorporating *Pam* [54,55]. Bioactive solutions were added in defined amounts to reach the target concentrations, and formulations containing the commercial biocide Econea® (E) were included for comparison (Table 1).

For lab-scale pre-validation of the *Pam*-functionalized coating formulations regarding AF properties, their ability to inhibit the settlement and/or thread production ability of *Mytilus galloprovincialis* larvae was evaluated in coated 24-well microplates for PU_*Pam* (0.35 and 0.7 wt%) and PDMS_*Pam* (0.7 wt%) formulations (Figure 2A).

PU marine coatings containing *Pam* seem to be effective against the settlement of mussel larvae on coated wells. PU_*Pam* 0.35wt% and 0.7 wt% formulations significantly inhibited larval settlement after 40 h (10 and 0% of larval settlement, respectively) when compared to the control (PU_C). PU_*Pam* 0.7 wt% formulation seems particularly effective as results show 0% larval settlement even after 15 h of exposure (Figure 2A). Regarding PDMS-based coating formulations, 0% of larval settlement was observed in the control (PDMS_C), which did not allow gauging the AF effect of *Pam*. This result is consistent with previous studies using lab-scale anti-settlement bioassays testing this base-coating [56–58] and emphasizes the fact that the matrix itself acts as a fouling release surface, as further supported by the more dynamic wettability behavior observed for the PDMS formulations (Figure S3 in the Supplemental information online).

Table 1. Coating formulations

[a]Coating	Polymeric matrix	Formulation		Average ratio of base/Curing agent (w/w)	Content in wet formulation (wt%)	
					Pam	Econea®
PU	Polyurethane	PU_C	+∴	8.9 ± 0.1	-	-
		PU_*Pam* (0.3 wt%)	+	8.8 ± 0.1	0.34 ± 0.01	-
		PU_*Pam* (0.7 wt%)	+∴	8.9 ± 0.1	0.72 ± 0.01	-
		PU_E	∴	8.8 ± 0.1	-	0.56 ± 0.01
PDMS	Polydimethylsiloxane	PDMS_C	+•∴	7.6 ± 0.1	-	-
		PDMS_*Pam* (0.3 wt%)	•	7.7 ± 0.1	0.33 ± 0.01	-
		PDMS_*Pam* (0.5 wt%)	•	7.7 ± 0.1	0.51 ± 0.01	-
		PDMS_*Pam* (0.7 wt%)	+•∴	7.7 ± 0.1	0.67 ± 0.01	-
		PDMS_E	∴	7.5 ± 0.1	-	0.56 ± 0.01

Formulations used in each experimental section are marked by the symbols: + larval settlement assays; • anti-biofilm assays; ∴ *in situ* prototypes.
[a]PU–polyurethane-based marine paint (F0032, Hempel A/S); Econea® (E) – 4-bromo-2-(4-chlorophenyl)-5-(trifluoromethyl)-1 H pyrrole-3-carbonitrile (biocide); PDMS–polydimethylsiloxane (PDMS)-based marine paint (Hempasil X3 +, Hempel A/S).

Regarding the byssal threads production endpoint (Figure 2A), for both the PU and PDMS coating matrices, test larvae were competent in their ability to produce byssal threads in all tested conditions. This observation validates the test conditions, as larvae seem to retain their settlement behavior by producing the structures for fixation but remain unable to attach to the selected coated surfaces, namely in PDMS and PU_*Pam* 0.7 wt% formulations.

Analysis of the seawater media used in the coated wells for the controls and *Pam*-functionalized formulations, by Liquid Chromatography-Mass Spectrometry (LC-MS), indicated that the leaching of *Pam* over the 40 h period was negligible for all the formulations tested (Figure S1 in the Supplemental information online).

The antibiofilm potential of *Pam*-functionalized PDMS coatings [PDMS_*Pam* (0.3 wt%), PDMS_*Pam* (0.5 wt%), and PDMS_*Pam* (0.7 wt%)] was evaluated under controlled hydrodynamic laboratory conditions after 49 days of cyanobacterial *Cyanobium* sp. LEGE 10375 biofilm development, and 14 days of bacterial *Cobetia marina* biofilm development. Only PDMS formulations were used in these bioassays, given the observed superior anti-settlement performance compared to PU formulations. Regarding cyanobacterial biofilms, quantitative and qualitative structural differences between biofilms formed on the different coating formulations and the control slide surfaces (Glass and PDMS_C) were analyzed by CLSM (Figure 2B). A reduction in the average biofilm biovolume was observed for all functionalized surfaces compared to glass (although with no statistically significant differences), and a significant effect was found for PDMS_*Pam* (0.7 wt%) compared to PDMS_C, reaching almost a 40% reduction (Figure 2B).

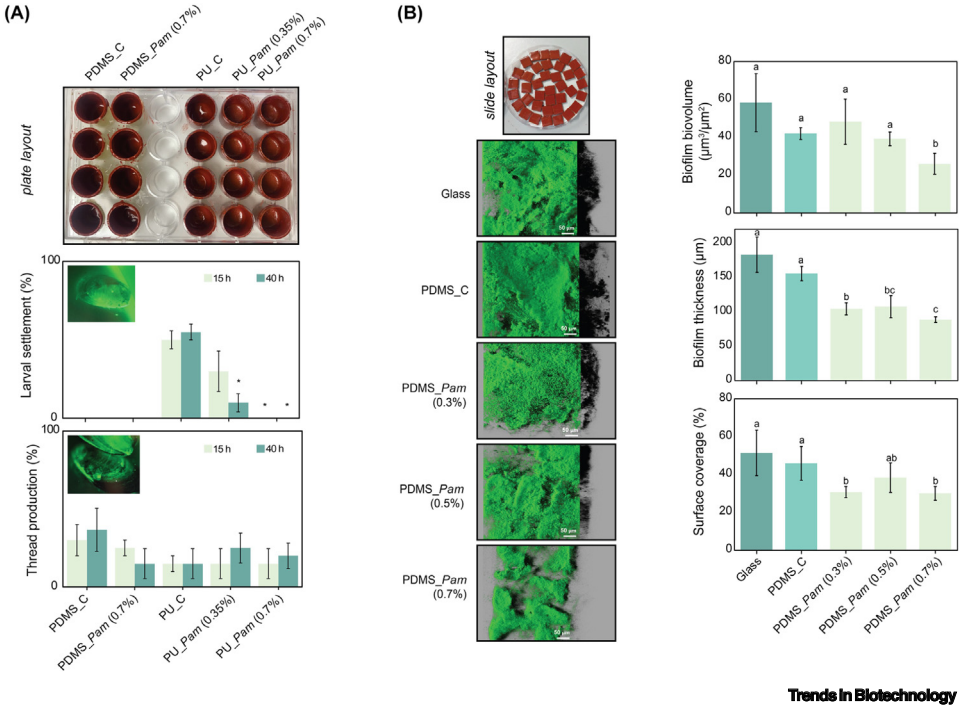

Figure 2. Antifouling performance of *Pam*-functionalized coating formulations in macro (A) and microfouling (B) bioassays. (A) Larval settlement and byssal threads production of *Mytilus galloprovincialis* larvae in the presence of the *Pam*-functionalized coating formulations (PDMS_*Pam* 0.7 wt%; PU_*Pam* 0.35 wt%, and PU_1 0.7 wt%) and control formulations (PDMS_C and PU_C); *indicates significant differences against the respective control formulation ($P < 0.05$, *t*-test). (B) Representative 3D cyanobacterial biofilm images and quantitative parameters (biofilm biovolume, biofilm thickness, and surface coverage) obtained from CLSM analysis of 49-day biofilms formed of *Cyanobium* sp. LEGE 10375 grown on control surfaces (glass and PDMS_C) and functionalized coatings (PDMS_*Pam* 0.3 wt%, PDMS_*Pam* 0.5 wt%, and PDMS_*Pam* 0.7 wt%). 3D images show the biofilm aerial view, with the virtual dark shadow projection on the right (illustrative of biofilm thickness). White scale bars are 50 µm. Means and standard deviations (SD) are shown (letters show statistical differences at $P < 0.05$, *t*-test).

Thinner *Cyanobium* sp. LEGE 10375 biofilms were formed on the functionalized coatings [PDMS_*Pam* (0.3 wt%), PDMS_*Pam* (0.5 wt%), and PDMS_*Pam* (0.7 wt%)] compared to those formed on Glass and PDMS_C with thickness reductions ranging from 30 to 43% compared to nonfunctionalized PDMS. Similar reductions in surface coverage were also observed on the functionalized coatings (Figure 2B). For all functionalized coatings [PDMS_*Pam* (0.3 wt%), PDMS_*Pam* (0.5 wt%), and PDMS_*Pam* (0.7 wt%)], a significant reduction in the total biofilm amount compared to control surfaces was observed.

Considering bacterial *C. marina* biofilms, a reduction in all parameters (biofilm total volume, biofilm thickness, and biofilm cells) was observed on PDMS_*Pam* (0.7 wt%) compared to PDMS_C (Figure S4 in the Supplemental information online). The biofilm biovolume decreased by up to 18% ($P < 0.05$) for PDMS_*Pam* (0.7 wt%) compared to PDMS_C (Figure S4A). Similar to what was observed with *Cyanobium* sp. LEGE 10375, thinner *C. marina* biofilms were developed on PDMS_*Pam* (0.7 wt%) compared to those formed on PDMS_C ($P < 0.05$), with overall reductions around 21% (Figure S4B). Moreover, a significant decrease in biofilm cell number was observed on PDMS_*Pam* (0.7 wt%), reaching an 82% reduction ($P < 0.05$; Figure S4C), confirming the antibiofilm potential of PDMS_*Pam* (0.7 wt%).

The performance of the foul-release silicone-based paint (PDMS_C) was previously evaluated for its potential to inhibit marine biofilm formation by common microfoulers [59,60]. Compared with a commercial epoxy resin used for hull coating, PDMS_C surfaces exhibited higher efficacy in decreasing biofilm formation during its maturation stage (from day 35 onward) [60]. These preliminary lab-scale anti-biofilm assays revealed that the most promising results against biofilms were obtained with *Pam*-functionalized PDMS at 0.7 wt%, showing significant reductions in biovolume, biofilm thickness, and surface coverage after 49 days of biofilm development, compared to biofilms formed on PDMS_C.

Overall, the potential of *Pam* after incorporation in coatings was confirmed in those anti-macro- and microfouling preliminary tests, which indicated that PU_*Pam* 0.7 wt% and PDMS_*Pam* 0.7 wt% formulations were the most promising formulations to be used in the *in situ* prototypes.

Pam-functionalized coating prototypes inhibit early biofilm formation, delaying hard biofouling community development under real marine conditions

Biological colonization of the test prototypes became visible after 2 months, showing distinct trends among formulations (Figure 3A; Table S6 in the Supplemental information online). By this time, PU_C and PU_E prototypes started to be colonized by a microbial biofilm, alongside early macrofoulers, visible by the presence of calcareous tubes of polychaeta (Annelida) and small colonies of erect hydrozoans (Cnidaria). After 3 months, biofilm coverage and thickness increased on PU_C and PU_E prototypes. In contrast, the PU *Pam*-functionalized coating prototype only showed polychaeta tubes, with a low-abundance biofilm appearing after 5 months (Figure 3A).

After 5 months, biofilm first appeared on the PU *Pam*-functionalized prototype, while macrofouling increased on the PU_C and PU_E prototypes (Figure 3A). These findings evidenced that PU *Pam*-functionalization effectively inhibited biofilm development for 5–7 months under real marine conditions, outperforming both the PU control and the commercial Econea®-based coatings. By month 7, microbial biofilms had developed across all PU formulations, while a thin biofilm started to form on the PDMS prototypes, with more noticeable colonization on the PDMS_C and PDMS_E prototypes (Figure 3A; see Table S6 in the Supplemental information online for detailed morpho-taxonomical analyses).

At 9 months, PU prototypes were colonized by a wide diversity of organisms (Figure 3A,B). PU_C exhibited abundant biofilm, a low abundance of polychaeta calcareous tubes, a few barnacles (Balanidae, Arthropoda), and erect hydroids. The PU_E prototype lacked hydrozoans but featured a colony of encrusting bryozoan *Watersipora subtorquata*. Surface coverage (ImageJ) analysis showed that PU_*Pam* had the lowest surface colonization (70.6%) with 29% free area, compared to PU_C (16%) and PU_E (14%) (Figure 3B). Even after 16 months, PDMS prototypes exhibited only a thin biofilm and sparse polychaeta calcareous tubes, along with a predominant encrusting sponge (*Halichondria* sp., Demospongiae, Porifera) in the PU_C prototype (Figure 3A,C; Table S6). PDMS coatings showed lower surface coverage than PU, with 62 and 44% for PDMS_*Pam* at 9 and 16 months, respectively (Figure 3B,C). At the end of the study (Figure 3C), PDMS formulations outperformed PU formulations, as expected, while differences in surface coverage among PU formulations (69–89%) were not significantly different. The time-dependent wettability measurements (Figure S3 in the Supplemental information online) further elucidate the distinct surface behaviors of PU- and PDMS-based coatings. PU formulations exhibited relatively stable contact angles over 600 s, indicating minimal dynamic changes in surface properties. In contrast, PDMS coatings showed more pronounced decreases in contact angles over time, consistent with hydrogel formation, surface reorganization, and the influence of

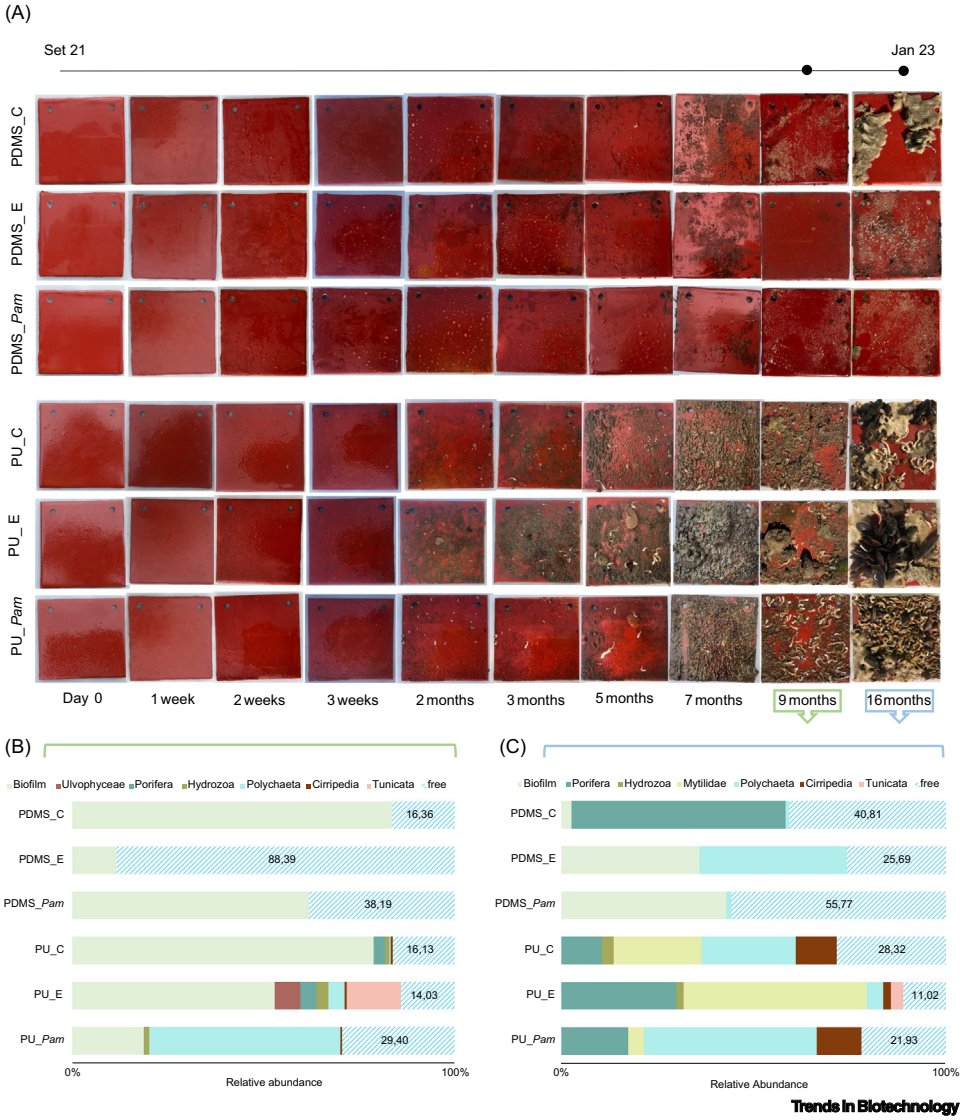

Figure 3. *In situ* biological colonization of the *Pam*-functionalized (PDMS_*Pam* and PU_*Pam*) prototypes, control formulations (PDMS_C and PU_C) and a positive control including the commercial antifouling agent Econea® (PDMS_E and PU_E). Temporal progression of biofouling communities (A); surface colonization (free area in the prototypes is represented by blue stripes as given by the ImageJ analyses), relative abundance (%), and morpho-taxonomic classification of prototypes communities 9 (B) and 16 (C) months after the first immersion.

incorporated additives such as *Pam*. These findings provide mechanistic insight into the higher time-dependent variability of PDMS surfaces relative to PU, which may contribute to the enhanced and sustained fouling-release performance of PDMS_*Pam* coatings during prolonged seawater exposure.

In summary, visual inspections and morpho-taxonomic analysis confirmed that *Pam*-functionalized formulations improved the efficacy of both PU and PDMS coatings in reducing biomass and diversity. These effects lasted up to 9 months for PU_*Pam* and persisted throughout the entire exposure period for PDMS_*Pam*, outperforming Econea®-based formulations.

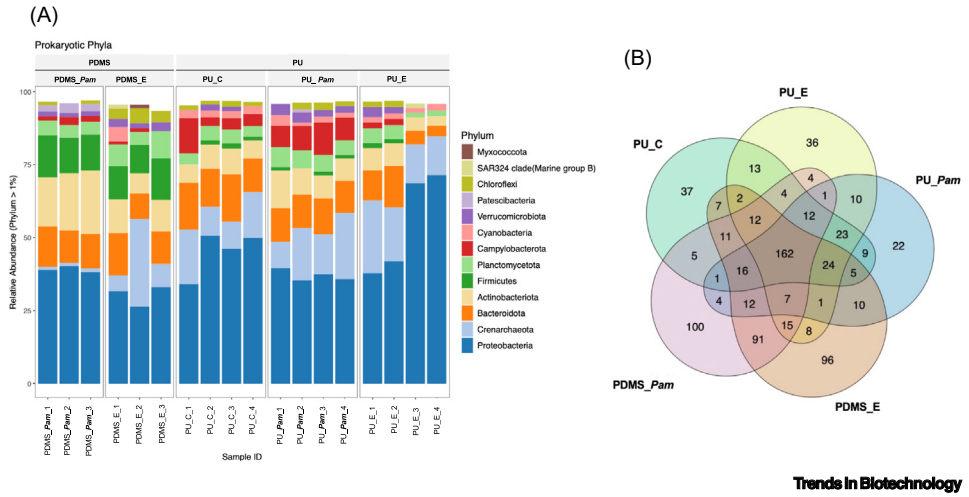

Figure 4. Prokaryotic community composition at the phylum level (A) and Venn diagram showing the number of exclusive and shared genera across the different treatments (B), determined by 16 S rRNA gene sequencing. Only phyla with relative abundance higher than 1% are shown in the stacked barplot.

Coating prototypes containing *Pam* show a significant effect on the structure of the early-stage biofouling community

The amplicon sequencing approach targeting prokaryotic and eukaryotic organisms in early-stage biofouling communities allowed the assessment of 12 112 amplicon sequence variants (ASVs) for the 16 S rRNA gene marker and 2402 ASVs for the 18S rRNA gene marker in test prototypes (Figures 4 and 5). No significant differences among treatments were observed regarding

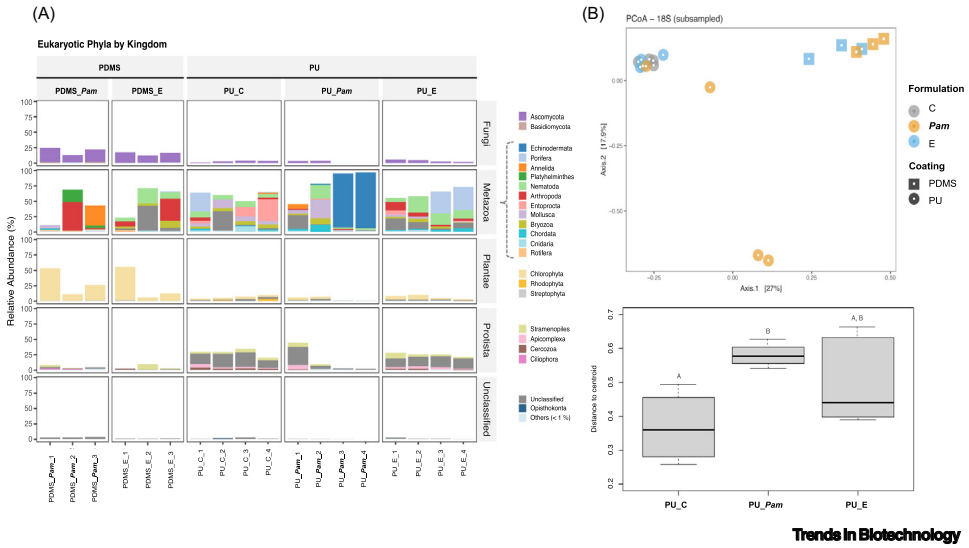

Figure 5. Eukaryotic community composition at the phylum level (A), β-diversity representation by a principal coordinate analysis (PCoA) plot (B), and boxplot representation of distances to centroid for prototypes treated with PU coating (C). The boxes represent the first and third quartiles, with median value bisecting each box. The whiskers extend to the largest/smallest value, excluding outliers (data beyond 1.5 inter-quartile range). Dissimilar letters in the boxplot of distances denote a significant difference between the formulations (one-way ANOVA, P <0.05). The effect of the coating matrix (R^2 = 0.25, P = 0.001) was stronger than that of the formulation (R^2 = 0.16, P = 0.006) in shaping eukaryotic community structure.

the effect of the coating formulations on prokaryotic species richness and α-diversity (Figure S5 in the Supplemental information online). Within the communities of the PDMS formulations, the species richness of the biofilm associated with the *Pam*-functionalized prototype was lower (1104 ± 32 ASVs) compared to the biofilm grown in the PDMS_E prototype (1224 ± 34 ASVs). Regarding the β-diversity of the same communities (Figure S6 in the Supplemental information online), significant effects of both the coating matrix and the formulation were detected (PERMANOVA, $P < 0.05$). There was a clear spatial separation between PU and PDMS coatings ($R^2 = 0.37$, $P = 0.001$) while the formulation appeared to have a finer effect on prokaryotic community dissimilarity ($R^2 = 0.13$, $P = 0.026$). The differences detected in prokaryotic β-diversity were visible in the taxonomic composition of these communities, even at the phylum level (Figure 4A). The major difference was observed in the relative abundance of Firmicutes, which was substantially higher in the biofilms grown on PDMS prototypes when compared to PU prototypes. Particularly in biofilms from the PDMS *Pam*-functionalized prototype (PDMS_*Pam*), an increase in the relative abundance of Firmicutes (129 ASVs) and also Actinobacteriota (153 ASVs) (12.9 and 19.4, respectively) was observed, together with a noticeable decrease in the relative abundance of Crenarchaeota (9 ASVs) and Cyanobacteria (14 ASVs) in this prototype (relative abundance of 1.1 and 0.57, respectively). Conversely, in the PU_*Pam* prototype, a decrease in the relative abundance of Firmicutes (1.1; 19 ASVs) was accompanied by an increase in the relative abundance of Campylobacterota (8.7; 28 ASVs).

According to the sequence analysis for all the prokaryotic genera present in the different prototypes (Figure 4B), PDMS_*Pam* prototype was the most favorable for microbial growth, given the detected number of exclusive genera (100), while PU_*Pam* showed the lowest (22).

When considering the eukaryotic communities, species richness and α-diversity were not significantly affected by the different coating matrix or formulation (Figure S7 in the Supplemental information online). Regarding β-diversity, a significant effect of the coating matrix and the formulation was observed in the eukaryotic communities, similar to what was observed for the prokaryotic communities (Figure 5, Table S7 in the Supplemental information online).

It is interesting to note that within the PU prototypes, the PU_C and PU_E formulations clustered very close to each other, while the PU_*Pam* formulation dispersed away from the PU cluster and had significantly greater beta dispersion than the control samples (Figure 5B). This observation strongly suggests that PU_*Pam* formulation has a significant effect on the eukaryotic community structure of the early colonizers.

In agreement with visual inspections, higher relative abundances of Fungi (Ascomycota) and Plantae (Chlorophyta) were detected in PDMS prototypes (Figure 5A), while higher relative abundances of protists and metazoans were detected in PU prototypes. In addition, within PU prototypes, PU_*Pam* was considerably less impacted by the higher abundance of protistan sequences (dominated by dinoflagellates) when compared to PU_C and PU_E formulations. Within the metazoan communities, a high intra-group variability was observed across all treatments, in particular for the PU_*Pam* prototype, where two of the replicates (PU_*Pam*_3 and PU_*Pam*_4) are dominated by Echinodermata. Only two Echinodermata ASVs were responsible for the drastic increase observed in these two samples; both are likely members of the genus *Antedon*, sessile crinoids that were not detected during visual inspections. This highlights, as previously advocated [61], that morphological identification of taxa should be complemented by metabarcoding analysis of important biofouling species, and vice versa.

Besides these overall and coarse trends, we also explored the treatment effects at the genus level for all eukaryotic kingdoms identified (Figure S8 in the Supplemental information online). Regarding fungal organisms, a higher number of different genera was detected in PDMS prototypes (15 genera >0.3%) than in PU (3 genera >0.3%). A higher number of different metazoan genera was detected in PU (35 genera >0.3%) than in PDMS (21 genera >0.3%) prototypes. Particularly, in the PDMS_*Pam* prototype, only seven metazoan genera were detected with relative abundances above 0.3%, in contrast to 15 detected in the PDMS_E prototype and 18 in PU_*Pam*. Among these seven, only four correspond to genera of known biofouling species, namely *Botryllus and Styela* (Tunicata), *Musculus* (Mytilidae), and *Lumbrineris* (Polychaeta). Notably, in the PDMS_*Pam* prototype, only polychaetes were identified in the visual morpho-taxonomical analysis, evidenced by the presence of a few scattered calcareous tubes. In contrast, nine genera associated with fouling communities were detected in PU_*Pam* (Figure S8), including *Mytilus* (Mytilidae), *Caberea, Membranipora*, and *Scrupocellaria* (Bryozoa), *Botryllus*, Molgula, and *Styela* (Tunicata), and *Eumida* (Polychaeta), although only *Mytilus* individuals and polychaeta tubes were observed in the visual assessment. Interestingly, no genera belonging to the *Balanidae* family (barnacles) were detected by the sequencing analysis in any prototype, despite their visual identification in PU-based formulations.

Regarding Plantae genera (Figure S8), *Prasiola*, one of the most abundant Plantae genera in this dataset, was substantially more abundant in PDMS than in PU prototypes. No apparent trends regarding formulation effects on Plantae genera were detected.

Overall, our results indicate that both *Pam*-containing formulations enhanced the AF performance of the prototypes, but through distinct and selective ecological mechanisms (Figure 6). The PU_*Pam* formulation significantly influenced the early eukaryotic community structure, privileging a specific macrofouling assemblage (metazoan, protistan, and plantae) while supporting a low microbial exclusive diversity (22ASVs). Visual analyses revealed that PU_*Pam* supports only a small subset of macrofouling species and minimal biofilm growth. However, the high relative abundance of metazoan genera detected through DNA-based HTS suggests potential inhibition of larval settlement and/or metamorphosis in response to certain chemical cues present. Campylobacterota-rich biofilms, such as those detected in PU_*Pam* prototypes, typically develop in sulfide- and redox-altered microenvironments and are associated with low oxygen, high sulfide, and variable pH, conditions that are generally unfavorable for larval settlement, which typically prefer more oxic and chemically stable surfaces [62]. This may explain the discrepancy between the reduced fouling diversity observed through morpho-taxonomic analysis and the higher richness revealed by sequencing, likely reflecting early colonizers that failed to successfully settle or metamorphose. In contrast, the PDMS_*Pam* formulation favored the establishment of microbial communities and exclusive genera, characterized by a high relative abundance of Firmicutes and Actinobacteria, and a reduced representation of Crenarchaeota and Cyanobacteria, while simultaneously deterring colonization of macrofouling taxa (metazoan). Members of the Firmicutes phylum, such as *Bacillus* and related genera, are known to produce antimicrobial peptides and biofilm-degrading enzymes, whereas Actinobacteria are prolific producers of antibacterial, anti-quorum sensing, and biofilm-inhibitory metabolites [63,64]. The ability of *Pam*-functionalized PDMS coatings to inhibit cyanobacterial biofilms was also validated under laboratory conditions in this study (Figure 2B). A biofilm dominated by Firmicutes and Actinobacteria, and lacking strong inductive settlement cues, such as extracellular polymeric substances (EPS) or secondary metabolites typically released by cyanobacteria or certain Gram-negative bacteria, may therefore contribute to inhibiting selected metazoan larval settlement [65–67].

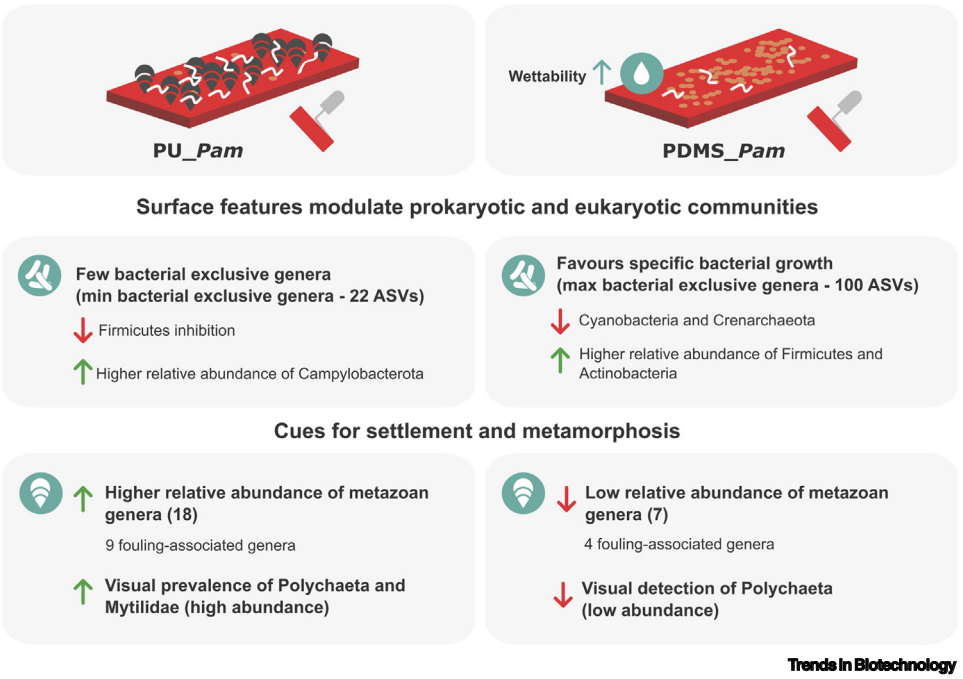

Figure 6. Putative selective ecological mechanisms underlying the differential behavior of *Pam*-engineered coating prototypes. The superior wettability of PDMS_*Pam* modulates the establishment of early colonizers, selecting specific prokaryotic phyla that favor biofilm growth, while limiting the abundance of macrofouling-associated genera. In contrast, PU_*Pam* supports only a few macrofouling species, as supported by visual analyses, and exhibits low biofilm development. The high relative abundance of metazoan genera detected by DNA-based high-throughput sequencing (HTS) may suggest settlement and metamorphosis impairment on PU_*Pam* prototypes.

Together, these selective microbial and ecological effects underscore the potential of *Pam* to modulate coating performance by limiting harmful macrofouling and shaping early biofilm community assembly.

Concluding remarks

In this study, the natural cyclic peptides *Pam*, derived from cyanobacteria and used as active ingredients in engineered coatings, act as effective antifouling mediators while posing minimal risk to marine ecosystems. ERA models predicted negligible impact, and lab-scale assays confirmed their ability to reduce cyanobacterial and bacterial biofilms' biovolume, thickness, and surface coverage, as well as to inhibit mussel larval settlement. *In situ* proof-of-concept tests further validated the antifouling effectiveness of *Pam*-functionalized PU and PDMS coatings, which delayed macrofouling colonization, outperforming control and commercial Econea® formulations. Overall, the integration of *Pam* as a bioactive ingredient in new engineered AF systems represents a technological advance from early proof-of-concept to near-application readiness (TRL 3–6), bridging the gap between laboratory innovation and near-application readiness (see Outstanding questions). Unlike conventional antifouling agents, which rely on toxic biocides with high environmental persistence and regulatory costs, this bio-based alternative combines high AF chemo-ecological efficacy with enhanced environmental safety, offering a sustainable alternative aligned with current regulatory and ecological priorities. Beyond environmental benefits, the use of natural, biodegradable active ingredients such as *Pam* may also reduce long-term operational and compliance costs, supporting the transition toward next-generation, eco-friendly antifouling technologies.

Outstanding questions

How can large-scale, cost-efficient, and sustainable production of cyanobacterial secondary metabolites, such as *Pam*, be optimized to support commercial antifouling applications?

How broadly effective are *Pam*-functionalized coatings across different biogeographic regions, seasons, and substrate types commonly found in ocean-related industries? And which environmental parameters most strongly influence their efficacy?

Can *Pam*-based formulations be further improved by integrating them with advanced polymer matrices or surface-engineering strategies to enhance durability, controlled *Pam* release, and compatibility with diverse end-user applications?

Which regulatory, standardization, and validation frameworks are needed to accelerate the transition from Technology Readiness Level 6 to market-ready, eco-safe marine antifouling technologies based on natural products?

Which molecular and chemo-ecological interactions enable *Pam*-based coatings to steer early biofouling assemblages toward an aggressive antifouling–effective biome? And can these mechanisms be generalized to engineer aggressive antifouling–effective biomes across diverse and dynamic marine environments?

STAR★METHODS

Detailed methods are provided in the online version of this paper and include the following:

- KEY RESOURCES TABLE
- METHOD DETAILS
  - Isolation and Purification of portoamides (*Pam*)
  - Ecotoxicity and environmental compatibility of *Pam*
    - Zebrafish Embryo Acute Toxicity Test
    - In silico predictions
  - Incorporation of *Pam* in polyurethane (PU) and polydimethylsiloxane (PDMS)-based coatings
  - Lab-scale antifouling experiments of *Pam*-functionalized coatings
    - Anti-settlement activity of Pam in polyurethane (PU) and polydimethylsiloxane (PDMS)-based coatings
    - Leaching assessment of Pam-functionalized coating formulations
    - Wettability measurements of Pam-functionalized coating formulations
    - Anti-biofilm properties of Pam polydimethylsiloxane (PDMS)-based coatings
  - Antifouling performance assessment of coated prototypes in real marine conditions
- QUANTIFICATION AND STATISTICAL ANALYSIS

Resource availability

Lead contact

Requests for further information and resources should be directed to, and will be fulfilled by, the lead contact, Joana R. Almeida (jalmeida@ciimar.up.pt; joana.reis.almeida@gmail.com).

Materials availability

Materials will be made available upon request from the lead contact, following standard Material Transfer Agreement (MTA) procedures.

Data and code availability

All data are available in the main text or in the supplemental information section. Raw data used to generate Figures 2 and 3 have been deposited in Zenodo (10.5281/zenodo.17648153). The 16 S and 18 S amplicon sequencing data, used to generate Figures 4 and 5, have been deposited in the European Nucleotide Archive (ENA) at EMBL-EBI under accession numbers PRJEB103959 (ERP185275) and PRJEB103962 (ERP185278), respectively. This paper does not report original code.

Author contributions

Conceptualization: J.R.A.; data curation: C.G., S.P., I.B.O., L.C.G., M.J.R, M.S., F.J.M., E.R.S., J.R.A.; methodology: C.G., S.P., I.B.O., M.P., J.M., L.C.G., M.J.R, M.S., F.J.M., V.V., E.R.S., J.R.A.; investigation: C.G., S.P., I.B.O., T.R., F.J.M., E.R.S., J.R.A.; resources: L.C.G., M.J.R, M.S., V.V., E.R.S., J.R.A.; validation: F.J.M., V.V., E.R.S., J.R.A; supervision: F.J.M., E.R.S., J.R.A; funding acquisition: J.R.A; writing—original draft: J.R.A.; writing—review & editing: all authors.

Acknowledgments

This research was funded by national funds through FCT - Fundação para a Ciência e a Tecnologia, I.P., and by the European Commission's Recovery and Resilience Facility, within the scope of CIIMAR UID/04423/2025 (https://doi.org/10.54499/UID/04423/2025), UID/PRR/04423/2025 (https://doi.org/10.54499/UID/PRR/04423/2025), and CIMAR LA/P/0101/2020 (https://doi.org/10.54499/LA/P/0101/2020), UID/04046/2023 - Biosystems and Integrative Sciences Institute and *NanoBioMitig* (https://doi.org/10.54499/2022.06149.PTDC), LEPABE (UID/00511/2025; https://doi.org/10.54499/UID/00511/2025; and UID/PRR/00511/2025; https://doi.org/10.54499/UID/PRR/00511/2025), and ALiCE (LA/P/0045/2020; https://doi.org/10.54499/LA/P/0045/2020).

This research was supported by the projects 2023.16744.ICDT, no. 17136 (COMPETE2030-FEDER-00853900) and no. 17414 (COMPETE2030-FEDER-01194000), funded by COMPETE2030 and PORTUGAL2030. This work was also supported by the Innovation Pact, Project No. C644915664-00000026 (WP2 Vertical Bivalves), under the 'Blue Bioeconomy

Pact', resulting from the submission of the application to Notice No. 02/C05-i01/2022, within the scope of the Recovery and Resilience Plan (PRR), co-funded by the Portuguese Republic and the EU, and by NORTE2030-FEDER-01796500, project co-funded by the EU through the NORTE 2030 Regional Program.

C.G. and S.P. acknowledge their PhD grants awarded (2022.12028.BD; https://doi.org/10.54499/SFRH/BD/145380/2019). J.R.A., I.B.O., and M.S. acknowledge their work contracts through the Scientific Employment Stimulus Individual Call (https://doi.org/10.54499/2022.03876.CEECIND/CP1728/CT0005, 10.54499/CEECIND/01368/2018/CP1574/CT0005, 10.54499/2023.08554.CEECIND/CP2848/CT0004, respectively).

The authors acknowledge support from the Blue Biotechnology and Ecotoxicology Culture Collection (LEGE-CC) at CIIMAR (https://lege.ciimar.up.pt) and Mariana Girão for graphical assistance.

Supplemental information

Supplemental information associated with this article can be found online at https://doi.org/10.1016/j.tibtech.2025.11.018.

References

1. Amara, I. *et al.* (2018) Antifouling processes and toxicity effects of antifouling paints on marine environment. A review. *Environ. Toxicol. Pharmacol.* 57, 115–130
2. Qian, P.-Y. *et al.* (2022) Marine biofilms: diversity, interactions and biofouling. *Nat. Rev. Microbiol.* 20, 671–684
3. Schultz, M.P. *et al.* (2011) Economic impact of biofouling on a naval surface ship. *Biofouling* 27, 87–98
4. Demirel, Y.K. *et al.* (2017) Effect of barnacle fouling on ship resistance and powering. *Biofouling* 33, 819–834
5. Galil, B.S. *et al.* (2019) *ICES Viewpoint background document: evaluating and mitigating introduction of marine non-native species via vessel bio- fouling*. ICES Ad Hoc Report 2019 17. https://doi.org/10.17895/ices.pub.14680
6. Lejars, M. *et al.* (2012) Fouling release coatings: a nontoxic alternative to biocidal antifouling coatings. *Chem. Rev.* 112, 4347–4390
7. Silva, E.R. *et al.* (2019) Eco-friendly non-biocide-release coatings for marine biofouling prevention. *Sci. Total Environ.* 650, 2499–2511
8. Kiosidou, E.D. *et al.* (2017) Rust morphology characterization of polyurethane and acrylic-based marine antifouling paints after salt spray test on scribed specimens. *J. Coat. Technol. Res.* 14, 1381–1395
9. Almeida, J.R. and Vasconcelos, V. (2015) Natural antifouling compounds: effectiveness in preventing invertebrate settlement and adhesion. *Biotechnol. Adv.* 33, 343–357
10. Faÿ, F. *et al.* (2023) Biobased anti-adhesive marine coatings from polyhydroxyalkanoates and polysaccharides. *Coatings* 13, 766
11. Holberg, S. *et al.* (2020) Hydrophilic silicone coatings as fouling release: simple synthesis, comparison to commercial, marine coatings and application on fresh water-cooled heat exchangers. *Mater. Today Commun.* 22, 100750
12. Donnelly, B. *et al.* (2022) Materials selection for antifouling systems in marine structures. *Molecules* https://doi.org/10.3390/molecules27113408
13. Paz-Villarraga, C.A. *et al.* (2022) Biocides in antifouling paint formulations currently registered for use. *Environ. Sci. Pollut. Res.* 29, 30090–30101
14. Carrier, A.J. *et al.* (2023) Transitioning towards environmentally benign marine antifouling coatings. *Front. Mar. Sci.* 10, 1175270
15. Pereira, D. *et al.* (2024) Proof of concept of natural and synthetic antifouling agents in coatings. *Mar. Drugs* 22, 291
16. Chen, L. *et al.* (2021) Biomimetic surface coatings for marine antifouling: natural antifoulants, synthetic polymers and surface microtopography. *Sci. Total Environ.* 766, 144469
17. Li, Z. *et al.* (2023) Bioinspired marine antifouling coatings: antifouling mechanisms, design strategies and application feasibility studies. *Eur. Polym. J.* 190, 111997
18. Harder, T. *et al.* (2004) A bacterial culture-independent method to investigate chemically mediated control of bacterial epibiosis in marine invertebrates by using TRFLP analysis and natural bacterial populations. *FEMS Microbiol. Ecol.* 47, 93–99
19. Sousa, M.L. *et al.* (2020) Portoamides A and B are mitochondrial toxins and induce cytotoxicity on the proliferative cell layer of *in vitro* microtumours. *Toxicon* 175, 49–56
20. Liu, M. *et al.* (2021) Research progress of environmentally friendly marine antifouling coatings. *Polym. Chem.* 12, 3702–3720
21. Cahill, P.L. *et al.* (2024) Creating new antifoulants using the tools and tactics of medicinal chemistry. *Acc. Chem. Res.* 57, 399–412
22. Neves, A.R. *et al.* (2024) A chemical toolbox to unveil synthetic nature-inspired antifouling (NIAF) compounds. *Mar. Drugs* 22, 416
23. Magin, C.M. *et al.* (2010) Non-toxic antifouling strategies. *Mater. Today* 13, 36–44
24. Satheesh, S. *et al.* (2016) Natural antifouling compound production by microbes associated with marine macroorganisms - A review. *Electron. J. Biotechnol.* 21, 26–35
25. Trepos, R. *et al.* (2014) Antifouling compounds from the subarctic ascidian synoicum pulmonaria: synoxazolidinones A and C, pulmonarins A and B, and synthetic analogues. *J. Nat. Prod.* 77, 2105–2113
26. Sjögren, M. *et al.* (2004) Antifouling activity of brominated cyclopeptides from the marine sponge geodia barretti. *J. Nat. Prod.* 67, 368–372
27. Labriere, C. *et al.* (2020) Phidianidine A and synthetic analogues as naturally inspired marine antifoulants. *J. Nat. Prod.* 83, 3413–3423
28. Liu, X. *et al.* (2024) Chemical signaling in biofilm-mediated biofouling. *Nat. Chem. Biol.* 20, 1406–1419
29. Leary, D.H. *et al.* (2014) Integrated metagenomic and metaproteomic analyses of marine biofilm communities. *Biofouling* 30, 1211–1223
30. Briand, J.F. *et al.* (2017) Spatio-temporal variations of marine biofilm communities colonizing artificial substrata including antifouling coatings in contrasted french coastal environments. *Microb. Ecol.* 74, 585–598
31. Antunes, J. *et al.* (2019) A multi-bioassay integrated approach to assess the antifouling potential of the cyanobacterial metabolites portoamides. *Mar. Drugs* 17, 111
32. Antunes, J. *et al.* (2019) Marine biofilms: diversity of communities and of chemical cues. *Environ. Microbiol. Rep.* 11, 287–305
33. Leão, P.N. *et al.* (2010) Synergistic allelochemicals from a freshwater cyanobacterium. *Proc. Natl. Acad. Sci. U. S. A.* 107, 11183–11188
34. Hoyberghs, J. *et al.* (2021) DMSO concentrations up to 1% are safe to be used in the zebrafish embryo developmental toxicity assay. *Front. Toxicol.* 3, 804033
35. Ribeiro, T. *et al.* (2017) Cytotoxicity of portoamides in human cancer cells and analysis of the molecular mechanisms of action. *PLoS One* 12, e0188817
36. TGD, E. (2003) *Technical guidance document on risk assessment in support of commission directive 93/67/EEC on risk assessment for new notified substances, Commission Regulation (EC) No 1488/94 on Risk Assessment for existing substances,*

and Directive 98/8/EC of the European Parliament and of the Council concerning the placing of biocidal products on the market. Part I–IV, European Chemicals Bureau (ECB), JRC-Ispra (VA), Italy
37. Oliveira, I.B. *et al.* (2014) Acute toxicity of tralopyril, capsaicin and triphenylborane pyridine to marine invertebrates. *Ecotoxicology* 23, 1336–1344
38. Antizar-Ladislao, B. (2008) Environmental levels, toxicity and human exposure to tributyltin (TBT)-contaminated marine environment. a review. b_antizar@hotmail.com. *Environ. Int.* 34, 292–308
39. Sousa, A.C.A. *et al.* (2014) History on organotin compounds, from snails to humans. *Environ. Chem. Lett.* 12, 117–137
40. Oliveira, I.B. *et al.* (2016) LC-MS/MS determination of tralopyril in water samples. *Chemosphere* 145, 445–449
41. Oliveira, I.B. *et al.* (2017) Toxicity of emerging antifouling biocides to non-target freshwater organisms from three trophic levels. *Aquat. Toxicol.* 191, 164–174
42. de Campos, B.G. *et al.* (2022) Occurrence, effects and environmental risk of antifouling biocides (EU PT21): are marine ecosystems threatened? *Crit. Rev. Environ. Sci. Technol.* 52, 3179–3210
43. Santos, J.V.N.D. *et al.* (2020) Can encapsulation of the biocide DCOIT affect the anti-fouling efficacy and toxicity on tropical bivalves? *Appl. Sci.* 10, 8579
44. Cai, Y. *et al.* (2021) Photochemical fate of medetomidine in coastal and marine environments. *Water Res.* 191, 116791
45. Fox, M. *et al.* (2014) The use of a corophium volutator chronic sediment study to support the risk assessment of medetomidine for marine environments. *Environ. Toxicol. Chem.* 33, 937–942
46. Hilvarsson, A. *et al.* (2009) Bioaccumulation of the new antifoulant medetomidine in marine organisms. *Mar. Environ. Res.* 68, 19–24
47. Lind, K.F. *et al.* (2013) Antioxidant and anti-inflammatory activities of barettin. *Mar. Drugs* 11, 2655–2666
48. Sjögren, M. *et al.* (2006) Antifouling activity of synthesized peptide analogs of the sponge metabolite barettin. *Peptides* 27, 2058–2064
49. Xu, Q. *et al.* (2022) Design, synthesis and *in vitro* biological evaluation of marine phidianidine derivatives as potential anti-inflammatory agents. *Bioorg. Med. Chem.* 71, 116936
50. Pereira, S. *et al.* (2025) Bioassay-guided discovery of antifouling nucleosides from the cyanobacterium leptothoe sp. LEGE 181152: efficacy, molecular targets, and ecotoxicological assessment. *Ecotoxicol. Environ. Saf.* 305, 119175
51. Pereira, F. *et al.* (2020) Antifouling napyradiomycins from marine-derived actinomycetes streptomyces aculeolatus. *Mar. Drugs* 18, 63
52. Wissner, J.L. *et al.* (2024) Novel metabolite madeirone and neomarinone extracted from streptomyces aculeoletus as marine antibiofilm and antifouling agents. *Front. Chem.* 12, 1425953
53. Pereira, S. *et al.* (2024) Antifouling activity and ecotoxicological profile of the cyanobacterial oxadiazine nocuolin A. *Chemosphere* 365, 143318
54. Silva, E.R. *et al.* (2021) Assessment of the environmental compatibility and antifouling performance of an innovative biocidal and foul-release multifunctional marine coating. *Environ. Res.* 198, 111219
55. Neves, A.R. *et al.* (2022) Antifouling marine coatings with a potentially safer and sustainable synthetic polyphenolic derivative. *Mar. Drugs* 20, 507
56. Vilas-Boas, C. *et al.* (2021) Multidimensional characterization of a new antifouling xanthone: structure-activity relationship, environmental compatibility, and immobilization in marine coatings. *Ecotoxicol. Environ. Saf.* 228, 112970
57. Resende, D. *et al.* (2021) From natural xanthones to synthetic C-1 aminated 3,4-dioxygenated xanthones as optimized antifouling agents. *Mar. Drugs* 19, 638
58. Rita Neves, A. *et al.* (2022) Gallic acid derivatives as inhibitors of mussel (mytilus galloprovincialis) larval settlement: lead optimization, biological evaluation and use in antifouling coatings. *Bioorg. Chem.* 126, 105911
59. Faria, S.I. *et al.* (2021) Unveiling the antifouling performance of different marine surfaces and their effect on the development and structure of cyanobacterial biofilms. *Microorganisms* 9, 1102
60. Faria, S.I. *et al.* (2020) Experimental assessment of the performance of two marine coatings to curb biofilm formation of microfoulers. *Coatings* 10, 893
61. Azevedo, J. *et al.* (2020) Monitoring of biofouling communities in a portuguese port using a combined morphological and metabarcoding approach. *Sci. Rep.* 10, 13461
62. Grosche, A. *et al.* (2025) The chemosynthetic biofilm microbiome of deep-sea hydrothermal vents across space and time. *Environ. Microbiome* 20, 88
63. Freckelton, M.L. *et al.* (2022) Bacterial lipopolysaccharide induces settlement and metamorphosis in a marine larva. *Proc. Natl. Acad. Sci. U. S. A.* 119, e2200795119
64. Muras, A. *et al.* (2021) Evaluation of the anti-fouling efficacy of *bacillus licheniformis* extracts under environmental and natural conditions. *Front. Mar. Sci.* 8, 2021
65. Dobretsov, S. and Rittschof, D. (2020) Love at first taste: induction of larval settlement by marine microbes. *Int. J. Mol. Sci.* 21, 731
66. Rajitha, K. *et al.* (2020) Role of bacterial biofilms and their EPS on settlement of barnacle (Amphibalanus reticulatus) larvae. *Int. Biodeterior. Biodegrad.* 150, 104958
67. Jagannathan, S.V. *et al.* (2021) Marine actinomycetes, new sources of biotechnological products. *Mar. Drugs* 19, 365
68. Callahan, B.J. *et al.* (2016) DADA2: high-resolution sample inference from illumina amplicon data. *Nat. Methods* 13, 581–583
69. McMurdie, P.J. and Holmes, S. (2013) phyloseq: an R package for reproducible interactive analysis and graphics of microbiome census data. *PLoS One* 8, e61217
70. Oksanen, J. *et al.* (2017) vegan: community ecology package. Software. http://CRAN.R-project.org/package=vegan
71. OECD (2013) T.N. 236: fish embryo acute toxicity (FET) test. *OECD Guidel. Test. Chem.* 2, 1–22
72. Maeder, V. *et al.* (2004) Toxic ratio as an indicator of the intrinsic toxicity in the assessment of persistent, bioaccumulative, and toxic chemicals. *Environ. Sci. Technol.* 38, 3659–3666
73. van Hattum, B. (2006) Emission estimation and chemical fate modelling of antifoulants. In *Antifouling Paint Biocides* (Konstantinou, I.K. *et al.*, eds), pp. 101–120, Springer Berlin Heidelberg
74. Oliveira, I.B. *et al.* (2016) Tralopyril bioconcentration and effects on the gill proteome of the mediterranean mussel mytilus galloprovincialis. *Aquat. Toxicol.* 177, 198–210
75. OECD (2004) *OECD environmental health and safety publications: series on emission scenario documents*
76. Callieri, C. (2008) Picophytoplankton in freshwater ecosystems: the importance of small-sized phototrophs. *Freshw. Rev.* 1, 1–28,28
77. Faria, S.I. *et al.* (2021) Developing new marine antifouling surfaces: learning from single-strain laboratory tests. *Coatings* 11, 90
78. Rossi, F. and De Philippis, R. (2015) Role of cyanobacterial exopolysaccharides in phototrophic biofilms and in complex microbial mats. *Life* 5, 1218–1238
79. Ramos, V. *et al.* (2018) Cyanobacterial diversity held in microbial biological resource centers as a biotechnological asset: the case study of the newly established LEGE culture collection. *J. Appl. Phycol.* 30, 1437–1451
80. Kotai, J. (1972) Instructions for preparation of modified nutrient solution Z8 for algae. *Nor. Inst. Water Res.* 11, 1–5
81. Romeu, M.J. *et al.* (2019) Biofilm formation behaviour of marine filamentous cyanobacterial strains in controlled hydrodynamic conditions. *Environ. Microbiol.* 21, 4411–4424
82. Alexandrou, A. (2001) *Principles of Fluid Mechanics*, Prentice Hall
83. Bakker, D.P. *et al.* (2003) Comparison of velocity profiles for different flow chamber designs used in studies of microbial adhesion to surfaces. *Appl. Environ. Microbiol.* 69, 6280–6287
84. Romeu, M.J. *et al.* (2024) Understanding the flow behavior around marine biofilms. *Biofilm* 7, 100204
85. Blain, S. *et al.* (2004) High frequency monitoring of the coastal marine environment using the MAREL buoy. *J. Environ. Monit.* 6, 569–575

86. Romeu, M.J. *et al.* (2023) Characterization and biofouling potential analysis of two cyanobacterial strains isolated from cape verde and Morocco. *FEMS Microbiol. Ecol.* 99, fiad004
87. Heydorn, A. *et al.* (2000) Quantification of biofilm structures by the novel computer program COMSTAT. *Microbiology* 146, 2395–2407
88. Romeu, M.J. *et al.* (2022) The use of 3D optical coherence tomography to analyze the architecture of cyanobacterial biofilms formed on a carbon nanotube composite. *Polymers* 14, 4410
89. Semedo, M. and Song, B. (2020) From genes to nitrogen removal: determining the impacts of poultry industry wastewater on tidal creek denitrification. *Environ. Sci. Technol.* 54, 146–157
90. Quast, C. *et al.* (2013) The SILVA ribosomal RNA gene database project: improved data processing and web-based tools. *Nucleic Acids Res.* 41, D590–D596
91. Guillou, L. *et al.* (2013) The protist ribosomal reference database (PR2): a catalog of unicellular eukaryote small sub-unit rRNA sequences with curated taxonomy. *Nucleic Acids Res.* 41, D597–D604

STAR★METHODS

KEY RESOURCES TABLE

Reagent or resource	Source	Identifier
Bacterial and virus strains		
Phormidium sp.	LEGE-CC	*Phormidium* sp. LEGE 05292
Cyanobium sp.	LEGE-CC	*Cyanobium* sp. LEGE 10375
Cobetia marina	DSMZ	*Cobetia marina* DSM 4741
Chemicals, peptides and recombinant proteins		
Econea® 4-bromo2-(4-chlorophenyl)-5-(trifluoromethyl)-1H-pyrrole-3-carbonitrile, 98%	Janssen	CAS#122454-29-9
N-methyl-2-pyrrolidone, 99.5%	Acros Organics (ThermoFisher Scientific)	**CAT#**445790025
Methyl ethyl ketone, >99.0%	Sigma-Aldrich	**CAT#**360473
Critical commercial assays		
QIAamp DNA Microbiome Kit	Qiagen	CAT#51704
Experimental models: Organisms/strains		
Danio rerio embryos	Lab stock	N/A
Mytilus galloprovincialis plantigrades	Memória Beach, Portugal	N/A
Oligonucleotides		
Primers: 16S V4–V5. Forward (515F): GTGCCAGCMGCCGCGGTAA Reverse (907R): CCGTCAATTCC TTTGAGTTT	Novogene	N/A
Primers: 18S V4 Forward (528F): GCGGTAATTCCAGCTCCAA Reverse (706R): AATCCRAGAATTTCACCTCT	Novogene	N/A
Software and algorithms		
MAMPEC v3.0	Deltares	https://www.deltares.nl/en/software-and-data/products/mampec
Prism V. v8.2.1	GraphPad	https://www.graphpad.com/features
dpiMAX	Dataphysics	https://www.dataphysics-instruments.com/products/oca/software/
IMARIS 9.1	Bitplane AG	https://imaris.oxinst.com/versions/9-1
COMSTAT	National Institutes of Health	www.comstat.dk
Fiji/ImageJ software v.1.54	National Institutes of Health	https://imagej.nih.gov/ij/
R v4.3.2 DADA2 v1.26 phyloseq v1.52.0 vegan v2.7-2	**-DADA2** [68] **-phyloseq** [69] **-vegan** [70]	https://www.r-project.org/ https://www.bioconductor.org/packages/release/bioc/html/dada2.html https://www.bioconductor.org/packages/release/bioc/html/phyloseq.html https://cran.r-project.org/web/packages/vegan/index.html
PASW Statistics 21.0	IBM	http://www.spss.com.hk/statistics/
Other		
Polyurethane F0038 paint base resin F0032 curing agent 95580	Hempel S/A	F0038 F0032 95580

(continued on next page)

(continued)

Reagent or resource	Source	Identifier
HEMPASIL X3+87500 paint Hempasil Base 87509 Hempasil Crosslinker 98951	Hempel S/A	CAT#87500
Universal tie-coat base resin XA17-17310 and curing agent XA18-RD003	Hempel S/A	XA17-17310 XA18-RD003
Acrylic substrates	Acrilcorte	N/A

METHOD DETAILS

Isolation and Purification of portoamides (*Pam*)

The cyanobacterial strain *Phormidium* sp. LEGE 05292 (LEGE-CC) was cultured in Z8 medium and upscaled to 100 l bioreactors (sleave bag), where it was grown for 6 months under 14 h light:10 h dark photoperiod (10–30 μmol photons $s^{-1}m^{-2}$), 25°C and air bubbling. After cell harvesting through centrifugation (*4700 rpm*), and lyophilization, the resulting biomass (99.5 g d.w.) was extracted with 100% methanol under constant stirring. The resulting crude extract (23.3 g d.w.) was fractionated by normal-phase, Vacuum Liquid Chromatography, and two reversed-phase chromatography steps to afford a 3:1 mixture of portoamides A and B (*Pam*, Figure 1 and Figure S1). Silica Gel 60, 0.015-0.040 mm, approximately 300 g), using the following solvent gradient: Fraction A: 500 ml of 10% hexane/90% ethyl acetate; Fraction B:500 ml 100% ethyl acetate; Fraction C: 500 ml 100% ethyl acetate; Fraction D: 500 ml 100% ethyl acetate; Fraction E: 500 ml 90% ethyl acetate/10% methanol; Fraction F: 500 ml 90% ethyl acetate/10% methanol; Fraction G: 500 ml 70% ethyl acetate/30% methanol; Fraction H: 500 ml 70% ethyl acetate/30% methanol; Fraction I: 500 ml 50% ethyl acetate/50% methanol; Fraction J: 500 ml 50% ethyl acetate/50% methanol; Fraction K: 1000 ml 100% methanol; Fraction L: 500 ml 100% methanol.

Fractions from J to L were confirmed by LC-MS/MS analysis to contain *Pam* and were thus further fractionated using a prepacked SPE C18 (50 g) cartridge as the stationary phase. The material adsorbed to the cartridge was eluted according to the following sequence: 150 ml 25% water/75% methanol; 150 ml 10% water/90% methanol; 250 ml 100% methanol; 200 ml 50% ethyl acetate/50% methanol; 100 ml 100% ethyl acetate; 50 ml dichloromethane; 100 ml 100% methanol; 50 ml ethyl acetate; 150 ml 100% methanol; 100 ml isopropanol. The eluate was collected in 10 ml glass tubes, the contents of which were pooled according to their TLC profiles, resulting in 17 fractions (fraction 1 to 17). Fractions 1 until 11 were confirmed to contain *Pam* by LC-MS/MS analysis (all eluted with methanol). These were subsequently merged (resulting in a mass of 4.7 g) and fractionated on Buchi Pure C-850 FlashPrep (Buchi Labortechnik AG, Flawil, Switzerland). Briefly, the sample was loaded onto a C18 column (220 g) with a flow of 50 ml/min, during 65 min, using a gradient program, from a mixture of 50% methanol/50% water, to 100% methanol and then to a mixture of 50% methanol/50% dichloromethane. The eluate was collected in 20 ml test tubes whose contents were pooled according to their UV (absorbance detector at 254, 265, 276, and 650 nm) and ELS profiles, resulting in 11 fractions (A to K). LC-MS/MS analysis confirmed that fraction D (1.1 g) contained a mixture of portoamides A and B (*Pam*) in a proportion of 3:1 (Figure S1 in the Supplemental information online). This defined mixture of naturally produced portoamides (*Pam*) was maintained and used in all the following experiments.

Ecotoxicity and environmental compatibility of *Pam*

Zebrafish Embryo Acute Toxicity Test. The OECD guideline 236 also known as Fish Embryo Acute Toxicity test (FET; OECD, 2013) [71], using zebrafish (*Danio rerio*) embryos, with modifications, was used to assess the lethal and sub-lethal effects of *Pam* [53]. The certified Bioterium of Aquatic Organisms (BOGA, CIIMAR, Porto) performed fish maintenance, breeding and embryo collection. All experiments were conducted in accordance with ethical guidelines of the European Union Council (Directive 2010/63/EU) and the Portuguese Ministry of Agriculture, Sea, Environment, and Spatial Planning (Decreto-Lei no. 113/7 August 2013) for the protection of animals used for experimental and other scientific purposes. Fish embryo exposures were conducted in E3 medium (pH 8.6), at 28°C, and adapted to 96-well plates. Briefly, ten newly fertilized eggs up to 1 h post fertilization (hpf) were exposed, per condition, to a range of concentrations (4.0 to 7.5 mg l^{-1}) of 1 until 96 hpf. Regular inspections of the embryos were performed under the microscope every 24 h, with solution renewal after each inspection. Indicators of lethality included coagulation of fertilized eggs, absence of heartbeat or somite formation, and failure of tail detachment from the yolk sac. Recorded sub-lethal endpoints included hatching time, tail deformities, presence of heart or yolk sac edema, and locomotion difficulties. Controls and solvent controls

(DMSO 0.1%) were included in the assays. Zebrafish experiments met the requirements for control survival and normal development of ≥90%. The assay was repeated three times. Zebrafish median lethal concentration (LC_{50}) estimates were obtained by nonlinear fitting to a four-parameter logistic equation through the least squares statistical method using Prism V. 8.2.1 (Graph Pad, CA, USA).

In silico predictions. The Toxicity Ratio, estimated LC_{50} vs the experimental LC_{50} value for a given species [72], was calculated to distinguish *Pam* between a baseline toxicant of a specifically toxic substance, as PBT (persistence, bioaccumulation, and toxicity) criteria of *Pam* are not available. The generated predictions were based on the molecular structure of the most abundant peptide of *Pam* - portoamide A. Input values included compound name, molecular weight, chemical formula [33] and SMILES notation. To understand the potential ecological risk of *Pam*, we used the Marine Antifoulant Model to Predict Environmental Concentrations (MAMPEC; Version 3.0; Deltares, Netherlands), by considering three different descriptors - environments, emission scenarios, and physicochemical properties [37,73,74] MAMPEC is able to calculate Predicted Environmental Concentrations (PEC), used for risk characterization (OECD-EU working group for the risk assessment of antifoulants) [75]. The worst-case scenario was used for risk characterization. Input values included the molecular formula and mass [33,35].

Incorporation of *Pam* in polyurethane (PU) and polydimethylsiloxane (PDMS)-based coatings

Commercial polyurethane (PU) and polydimethylsiloxane (PDMS)-based marine polymeric matrices were used to prepare and optimize coating formulations incorporating *Pam*, according to previously developed methodologies [54,55]. To enhance compatibility and ensure homogeneous formulations, *Pam* was first dissolved in *N*-methyl-2-pyrrolidone (NMP, 99.5%, Acros Organics, Geel, Belgium) at *Pam*/solvent ratios of 0.06 ± 0.01, and 0.04 ± 0.01 for PU- and PDMS-based formulations, respectively. These bioactive solutions were blended into two distinct bi-component coating systems: a PU-based system comprising base resin F0032 and curing agent 95 580 (Hempel, A/S, Copenhagen, Denmark), and a foul-release PDMS-based coating system, HEMPASIL X3 + 87 500 paint (Hempel, A/S, Copenhagen, Denmark), which consists of a base resin (reference 87509) and a curing agent (reference 98950). The bioactive solutions were added in exact amounts to achieve the desired contents in the wet formulation systems (Table 1).

For comparison purposes, coating formulations containing the commercial biocide Econea® (E) were prepared. Biocide E was firstly dissolved in methyl ethyl ketone (MEK, >99.0%, Sigma-Aldrich) to obtain biocidal solutions with a biocide/solvent ratio of 0.45 ± 0.02. The resulting biocidal solutions were then incorporated into the bi-component PU- and PDMS-based coating systems, following the same procedure described above.

The optimized coating formulations were further applied to coat several acrylic substrates (Acrilcorte, Portugal) for lab-scale assessment of anti-settlement (mussel larvae) and anti-biofilm activities, as well as antifouling performance under real marine conditions, following the procedure recommended by the paint supplier Hempel A/S.

For the larval settlement assessment, 24 well-acrylic plates (4 wells/formulation) were coated using conventional brush painting [56]. Coated acrylic slides (1 cm^2, 100 slides/formulation) and larger prototypes (10 cm^2) for lab-scale anti-biofilm testing and real marine antifouling performance assessments, respectively, were prepared using a four-sided film applicator (300 μm) with a reservoir (TQC Sheen). Formulations selected for each of the antifouling assessment experiments are indicated in Table 1.

Specifically, for the PDMS-based formulations, substrates were pre-coated with a universal tie-coat (base resin XA17-17310 and curing agent XA18-RD003), followed by an 8-h curing step at room temperature (approximately 23°C). After this step, a second coating with the HEMPASIL X3 + system was applied, with an additional curing step of about 1 weeks to ensure the complete curing. For PU-based formulations, substrate coating involved a single coating step and curing at room temperature (approximately 23°C) for about 1 weeks.

Lab-scale antifouling experiments of *Pam*-functionalized coatings

Anti-settlement activity of Pam in polyurethane (PU) and polydimethylsiloxane (PDMS)-based coatings. For a preliminary efficacy assessment of the coating formulations, *Mytilus galloprovincialis* plantigrade larvae were used to evaluate their ability to settle in the presence of the different coatings under laboratory-controlled conditions. Larvae were collected from Memória beach (N41°13′51.5″, W8°43′15.5″) at low tide. Competent plantigrades with exploring behaviour (i.e., moving their foot searching for the appropriate substrate to settle) were selected in the laboratory and transferred to the coated wells with different formulations (PU and PDMS).

All the coated wells were filled with filtered natural seawater to reduce any interferents. The coating formulations (PU_*Pam* 0.3, and 0.7 wt.% and PDMS_*Pam* 0.7 wt.%) were tested in four replicates (wells) with five plantigrades per well with a total of 20 larvae per treatment. A negative control (base coating) was included. After 15, and 40 h, the percentage of larval settlement as well as thread production was determined by the presence/absence of efficiently attached byssal threads (on the surface of the coating or within larvae) produced by each individual in each formulation condition. Larvae that did not settle (i.e., did not produce byssal threads) remained alive during the assays, but unattached to the substrate throughout the assay period. The best-performing polymeric matrix was selected for further lab-scale analysis on anti-biofilm properties.

Leaching assessment of Pam-functionalized coating formulations. After 40 h of exposure, seawater from the coated wells containing *Pam*-functionalized formulations (PU_*Pam* 0.35% and 0.7 wt.% and PDMS_*Pam* 0.7 wt.%) and controls (PU_C and PDMS_C) were analysed by LC-MS. Negative (blanks) and a positive control containing *Pam* were included. Samples were injected in a Liquid Chromatograph Thermo Finnigan Surveyor HPLC System (Thermo Scientific, MA, USA), coupled to a Mass Spectrometry LCQ Fleet™ Ion Trap Mass Spectrometer (Thermo Scientific, MA, USA). Data were acquired and processed is XcaliburTM version 2. Mass Spectrometer Tune Method parameters optimization was performed through direct injection of purified portoamides A, B, C and D (~5 µg/ml) dissolved in Methanol (0.1% formic acid). The Mass Spectrometer operated in electrospray positive polarity mode using *Single Ion Monitoring* (SIM). The spray voltage was maintained at 3.50 kV; Capillary temperature at 275°C; Capillary voltage and tube lens maintained at 300, and 120 kV, respectively. Nitrogen was used as sheath and auxiliary gas and helium as a buffer. Separation was achieved on an ACE Excel C18 (50 × 2.1 mm I.D., 1.7 µm, Batch: V17-1253, Avantor® ACE ®) kept at 35°C, with a flow rate of 0.25 ml/min. and injected volume was 10 µl in a no waste mode. The eluents used were methanol (A) and water (B) both acidified with formic acid at 0.1% (v/v). The gradient program started at 45% A, increasing to 90% A in 8 min, returning to initial conditions in 5 min, and equilibrating for 8 min with 45% A.

Wettability measurements of Pam-functionalized coating formulations. Wettability is a key surface property supporting the antifouling behavior of different polymeric matrices and was evaluated to understand the influence of *Pam* incorporation on the original wettability properties of coatings. The influence of *Pam* on the surface wettability of PDMS and PU coatings was evaluated through wettability tests performed on coated acrylic substrates (10 × 10 mm) by monitoring the hydrophobicity of the developed coating formulations (static water contact angle over time). Static contact angle measurements were recorded over time using the sessile drop method, following the ASTM standard D5725-99 (2003). The sessile drop method was applied at 25°C, and images were recorded and analyzed from 0 to 600 s using a contact angle meter (Dataphysics OCA 25, Filderstadt, Germany) and dpiMAX software. Water contact angle values represent the average of at least 10 independent measurements per formulation.

Anti-biofilm properties of Pam polydimethylsiloxane (PDMS)-based coatings. *Cyanobium* sp. LEGE 10375 (Synechococcales order) was used as a model marine bacterium to study the antifouling performance of the functionalized coatings at laboratory scale. This picocyanobacterium has been used in marine biofouling studies due its strong biofilm-forming capacity and ecological relevance [59,60,76,77]. Cyanobacteria are dominant constituents of marine phototrophic biofilms, known for initiating biofilm formation and secreting large amounts of extracellular polymeric substances (EPS), which contribute significantly to biofilm structure and resilience [78]. Additionally, members of the Synechococcales order, including *Cyanobium* sp., are widely distributed across diverse geographic regions (Africa, America, Antarctica, and Europe) and thrive in marine, brackish, and freshwater environments [76]. Together with *Synechococcus, Cyanobium* represents one of the dominant picocyanobacterial genera in these ecosystems [76,79]. The *Cyanobium* sp. LEGE 10375 strain was obtained from the Blue Biotechnology and Ecotoxicology Culture Collection (LEGE-CC) [79]. Bacterial cells were grown in 750 ml of Z8 medium supplemented with 25 $g.l^{-1}$ of synthetic sea salts (Tropic Marin) and vitamin B_{12} (Sigma Aldrich, Merck, Saint Louis, MO, USA) [80]. Cultures were incubated under a cycle of 14 h of light (10–30 µmol photons/m^2/s), followed by 10 h of darkness at 25°C [81].

Cyanobacterial biofilm development was performed using 12-well microtiter plates (VWR International) in a long-term assay under controlled hydrodynamic conditions to mimic marine environments [81]. Borosilicate glass slides (1 cm^2) were used as pristine control surfaces. The PDMS_C coated slides (negative control), *Pam*-functionalized coatings (PDMS_ *Pam* (0.3 wt.%), PDMS_*Pam* (0.5 wt.%), PDMS_*Pam* (0.7 wt.%)), and glass slides were sterilized by ultraviolet radiation for 30 min before use. After fixing the surfaces with double-sided adhesive tape to 12-well microtiter plates, 3 ml of the adjusted cyanobacterial suspension at a final concentration of 1 × 10^8 cells ml^{-1} was added into each well, and the microtiter plates were incubated at 25°C and 185 rpm in an orbital shaker

with a 25 mm diameter (Agitorb 200ICP, Norconcessus). In this platform, an average shear rate of 40 s^{-1} is achieved at the beginning of biofilm formation, which is similar to the values of shear rate that a ship in a harbor is subjected to (50 s^{-1}) [82,83]. During biofilm development, the shear rates at the biofilm surface were shown to depend on the biofilm architecture [84]. Biofilm development was followed for 49 days (seven weeks) since it is accepted that a two-month interval for maintenance is the minimum period for economically viable underwater monitoring systems [81,85]. During this time, the medium was replaced twice a week, and to mimic real light exposure periods, a photoperiod of 14 h light (8–10 µmol photons m^{-2} s^{-1})/10 h dark cycles was applied.

After 49 days of biofilm development, cyanobacterial biofilms formed on the control surfaces (Glass and PDMS_C), and the *Pam*-functionalized coatings (PDMS_*Pam*) were analyzed by confocal laser scanning microscopy (CLSM). Coupons were removed from the microplates, washed with saline solution, and the biofilms were stained for 10 min with 6 µm cell-permeant nucleic acid marker SYTO®9 (Thermo Fisher Scientific, Waltham, MA, USA). Each stained biofilm was mounted on a microscopic slide and image acquisition was performed using a Leica TCS SP5 II confocal laser scanning microscope (Leica Microsystems, Wetzlar, Germany) with a 40 × water objective lens (LEICA HCX PL APO CS 40.0x/1.10WATER UV) [60,77,86]. Three-dimensional (3D) projections of the biofilms were constructed from the CLSM acquisitions using the 'Easy 3D' function of the IMARIS 9.1 software (Bitplane, Zurich, Switzerland). Additionally, biofilm structural parameters such as biovolume ($\mu m^3/\mu m^2$), biofilm thickness (µm), and surface coverage (%) were determined using COMSTAT image analysis software (National Institutes of Health, Bethesda, MD, USA) [87]. A minimum of five stacks of horizontal-plane images (512 × 512 pixels, corresponding to 387.5 µm × 387.5 µm) with a z-step of 1 µm were acquired per sample, and a total of three samples coming from two biological assays were analyzed (n=6).

To expand the microbial scope of the anti-biofilm assays, the marine heterotrophic bacterium *Cobetia marina* DSM 4741 was tested as an additional microfouler organism. Colonies of *C. marina*, previously grown on the salt-rich Våatanen Nine Salt Solution (VNSS) marine medium supplemented with 15 g/l agar (VWR International, Leuven, Belgium), were inoculated into 100 ml of liquid VNSS medium. After overnight incubation at 25°C and 120 rpm (Agitorb 200ICP, Norconcessus, Ermesinde, Portugal), the bacterial suspension was centrifuged for 10 min at 3100 × *g* (Eppendorf Centrifuge 5810R, Eppendorf, Hamburg, Germany). The resulting pellet was resuspended in fresh VNSS medium and adjusted to a final concentration of 1 × 10^8 cells/ml prior to biofilm formation assays.

Biofilm development was assessed on PDMS_C-coated slides (control) and on the most promising *Pam*-functionalized coating (PDMS_*Pam* (0.7 wt.%)) under the same conditions. Biofilms were allowed to develop over 14 days, with the culture medium replaced twice weekly. After 14 days, biofilms were characterized using Optical Coherence Tomography (OCT) to quantify biofilm thickness and total volume, while the number of biofilm cells was determined by colony-forming unit (CFU) enumeration. The culture medium was removed, and the microplate wells were gently rinsed with sterile saline solution (8.5 g/l NaCl) to eliminate loosely attached cells. Fresh sterile saline was then added, and 3D OCT acquisitions were performed using a Thorlabs Ganymede Spectral Domain OCT system with a central wavelength of 930 nm (Thorlabs GmbH, Dachau, Germany) [81]. Image analysis and quantification of biofilm parameters were performed [88]. Following imaging, biofilms were detached from the surfaces by immersing the coupons in 2 ml of sterile saline and vortexing for 3 min. The resulting bacterial suspensions were serially diluted and plated on VNSS agar, followed by overnight incubation at 25°C for CFU enumeration.

Antifouling performance assessment of coated prototypes in real marine conditions

For the analyses of biological colonization in real sea conditions, prototypes (10 × 10 cm) coated with PU and PDMS-based marine coating formulations containing *Pam*, the commercial AF agent Econea® and correspondent controls were subjected to immersion tests at a pier in the cruise ship terminal of the Leixões Port, Matosinhos, Portugal (41° 11' N 8° 42' W), in accordance with ASTM D6990 and D3623-78a standards. The *in situ* test was performed from September 2021 to January 2023. Nine timepoints of inspection were applied including weekly inspections for the first month, and then after 2, 3, 5, 7, 9, and 16 months of submersion. During inspections, photographic records of all the prototypes and environmental parameters data were recorded. Biological samples of the biofouling community (biofilm and surface first colonizers) were collected from each prototype according to the level of colonization for each formulation over time. For the PU-coating prototypes, biological

samples (4 replicates) were collected by gentle scratching from the surface of the prototypes in the timepoint 8 (after 9 months of submersion). For the PDMS-coating prototypes (3 replicates), the same procedure was only possible after 16 months of exposure due to the intrinsic antifouling properties of the PDMS matrix and was conducted only for the PDMS_E and PDMS_*Pam* formulations. All prototypes were permanently immersed throughout the duration of the test (16 months).

At the sampling site and for all time points, seawater physical-chemical parameters such as temperature (°C), salinity, dissolved oxygen concentration (mg l^{-1}), oxygen saturation (%), and pH were measured, with calibrated multiparametric probes (HI98194 Hanna Instruments). Field tests were carried out under an average pH of 7.78 and a salinity ranging from 24 to 38%, for a water depth of 1.5 to 3 m, with temperatures ranging from 13 to 21 °C, and for a test period of 16 months to include all-season conditions (Table S1 in the Supplemental information online).

Photographic records of the prototypes from inspections at different time points were analyzed to determine biomass coverage percentages using Fiji/ImageJ software v.1.54. *In situ* registrations and prototype images were also used for a qualitative assessment of predominant fouling taxa throughout the study. Taxa were classified according to the World Register of Marine Species (WoRMS) nomenclatural system (WoRMS Editorial Board, 2021).

The biological samples of the early-stage biofouling community were used to investigate the microbial and early macrobiota community composition and diversity by high-throughput sequencing (HTS) of the 16S and 18S rRNA genes, which are universal markers for prokaryotic and eukaryotic taxonomic classification, respectively. Total DNA was extracted using commercial extraction kits (QIAamp DNA Microbiome Kit, Qiagen). Extracted DNA was prepared for Illumina MiSeq PE250 sequencing by PCR amplification of hypervariable regions of 16S (V4-V5) and 18S (V4) rRNA genes, using the primers 515F (5'-GTGC CAGCMGCCGCGGTAA-3')/907R (5'-CCGTCAATTCCTTTGAGTTT-3') and 528F (5'-GCGGTAATTCCAGCTCCAA-3'/706R (5'-AATCCRAGAATTTCACCTCT-3'), respectively (Table S2 in the Supplemental information online).

The raw FASTQ files obtained with Illumina MiSeq were trimmed for primer and barcode removal and imported into R, using the dada2 package [68]. Sample filtering, dereplication, amplicon sequence variant (ASV) inference, merging, and chimera removal were performed with default settings for both 16 S and 18 S reads, similarly to previously described [89]. These pre-processing steps resulted in a mean number of 22 305 16S reads and 44 627 18S reads per sample (Table S3 in the Supplemental information online), corresponding to a total of 12 112 and 2402 ASVs, respectively. Prokaryotic taxonomy was assigned on the 16S final reads using the dada2 naive Bayesian classifier with the Silva v138 reference database [90]. Taxonomy filtering was applied to the 16S reads by removing eukaryotic, mitochondrial, and chloroplast sequences (201 ASVs were removed). Eukaryotic taxonomy was assigned on the 18 S final reads using the same dada2 classifier with the Silva v132_18 S reference database [90]. Additionally, for disambiguation of some taxa classification, eukaryotic taxonomy was further classified with the PR2 v4.14.0 database [91] and through an NCBI blast on the Core Nucleotide Database (core_nt). Relative abundances of each ASV per sample were calculated in the filtered 16 S and 18 S datasets by dividing the absolute abundance (counts) of each ASV by the sum of counts of all ASVs, using the phyloseq package [69]. The number of observed ASVs per sample and the Shannon index were used to estimate species richness and α-diversity, respectively. Differences in species richness and α-diversity between the different treatments were tested with a two-way analysis of variance (ANOVA, coating matrix and formulation as categorical factors) and a Tukey's HSD test to perform multiple comparisons. β-diversity among samples was estimated with the Bray-Curtis dissimilarity calculator and a principal coordinate analysis (PCoA). Significant effects of coating matrix and formulation on community dissimilarity were tested by a non-parametric permutational ANOVA (PERMANOVA) using the adonis function of the vegan package in R [70]. Multivariate homogeneity of group dispersion was evaluated using the betadisper function of the same R package. To normalize α- and β- diversity estimates, samples were randomly subsampled to the lowest number of sequences per sample in each dataset.

QUANTIFICATION AND STATISTICAL ANALYSIS

Biological and environmental data were presented as means with standard deviations or as individual observations. Normality and variance equality were assessed using Kolmogorov-Smirnov and Levene's tests, with appropriate data transformations applied when assumptions were not met. Independent unpaired t-tests (α=0.05, $p < 0.05$) were used to compare lab-scale anti-settlement test results and qualitative biofilm parameters. Statistical analyses were conducted using PASW Statistics 21.0.

LC values for zebrafish were estimated through nonlinear regression using a four-parameter logistic model with least-squares fitting in Prism v8.2.1 (GraphPad, CA, USA).

Analysis and downstream processing of DNA sequencing data were conducted within the R statistical computing environment.